0022-3565/11/3393-896–904$25.00
THE JOURNAL OF PHARMACOLOGY AND EXPERIMENTAL THERAPEUTICS
JPET 339:896–904, 2011

Vol. 339, No. 3
185686/3730724
Printed in U.S.A.

Modeling Diabetes Disease Progression and Salsalate Intervention in Goto-Kakizaki Rats

Yanguang Cao, Debra C. DuBois, Hao Sun, Richard R. Almon, and William J. Jusko

Department of Pharmaceutical Sciences, School of Pharmacy and Pharmaceutical Sciences (Y.C., D.C.D., H.S., R.R.A., W.J.J.), and Department of Biological Sciences (D.C.D., R.R.A.), State University of New York, Buffalo, New York

Received July 1, 2011; accepted September 8, 2011

ABSTRACT

Type 2 diabetes mellitus (T2DM) arises owing to insulin resistance and β-cell dysfunction. Chronic inflammation is widely identified as a cause of T2DM. The Goto-Kakizaki (GK) rat is a spontaneous rodent model for T2DM with chronic inflammation. The purpose of this study was to characterize diabetes progression in GK rats and evaluate the potential role of the anti-inflammatory agent salsalate. The GK rats were divided into control groups ($n = 6$) and salsalate treatment groups ($n = 6$), which were fed a salsalate-containing diet from 5 to 21 weeks of age. Blood glucose and salicylate concentrations were measured once a week. Glucose concentrations showed a biphasic increase in which the first phase started at approximately 5 weeks, resulting in an increase by 15 to 25 mg/dl and a second phase at 14 to 15 weeks with an upsurge of more than 100 mg/dl. A mechanism-based model was proposed to describe the natural diabetes progression and salsalate pharmacodynamics by using a population method in S-ADAPT. Two transduction cascades were applied to mimic the two T2DM components: insulin resistance and β-cell dysfunction. Salsalate suppressed both disease factors by a fraction of 0.622 on insulin resistance and 0.134 on β-cell dysfunction. The substantial alleviation of diabetes by salsalate supports the hypothesis that chronic inflammation is a pathogenic factor of diabetes in GK rats. In addition, body weight and food intake were measured and further modeled by a mechanism-based growth model. Modeling results suggest that salsalate reduces weight gain by enhancing metabolic rate and energy expenditure in both GK and Wister-Kyoto rats.

Introduction

Type 2 diabetes mellitus (T2DM) develops as a consequence of an interplay between peripheral insulin resistance and β-cell dysfunction. Insulin resistance is an early abnormality that is usually attributed to obesity. During the prediabetic period, the presence of insulin resistance does not initiate a noticeable glucose increase in plasma because of β-cell adaptation that permits the maintenance of normal glucose metabolism. However, pancreas β-cell function will gradually decline over time, and this adaptation will eventually fail, owing to both genetic and environmental factors. Overt T2DM will appear. Growing evidence supports decreased functional β-cells as the hallmark of T2DM (Marchetti et al., 2006).

T2DM is a syndrome that has been defined as "a group of metabolic disorders," which indicates that T2DM has a multifactorial pathogenesis, including genetic, epigenetic, and environmental factors. Several lines of evidence suggest that T2DM is highly associated with a generalized activation of the innate immune system, in which a chronic and systematic low-grade inflammation is involved (Wellen and Hotamisligil, 2005). Chronic inflammation can cause insulin resistance in adipose tissue, skeletal muscle, and liver by inhibiting insulin signaling via autocrine/paracrine/endocrine pathways (Olefsky and Glass, 2010). Chronic inflammation in islet cells has been characterized by the presence of cytokines, immune cells, and amyloid deposits, which contribute to the decrease in β-cell mass and the impaired function (Donath et al., 2009; Ehses et al., 2009a). Further evidence for roles of chronic inflammation in T2DM comes from clinical studies using either anti-inflammatory approaches or biological agents that target specific proinflammatory cytokine pathways to improve parameters of glucose control especially with IL-1β antagonism and salsalate treatment (Larsen et al., 2007; Goldfine et al., 2008).

The application of model-based approaches to gain insight into disease progression is widely accepted in the field of diabetes and antidiabetic drug development (Gobburu and Lesko, 2009). However, human T2DM often takes years to

This research was supported by the National Institutes of Health National Institute of General Medical Sciences [Grant GM57980] and the University of Buffalo-Pfizer Strategic Alliance.
Article, publication date, and citation information can be found at http://jpet.aspetjournals.org.
doi:10.1124/jpet.111.185686.

ABBREVIATIONS: T2DM, type 2 diabetes mellitus; GK, Goto-Kakizaki; WKY, Wister-Kyoto; NF, nuclear factor; IL, interleukin; BW, body weight; LBM, lean body mass; SE%, relative standard error.

develop, and it is costly to assess the effect of interventions on the whole process of clinical diabetes. Animal models allow interventions to be assessed in much shorter time spans. Goto-Kakizaki (GK) rats provide a polygenic model for spontaneous T2DM by inbreeding Wister rats with glucose intolerance for more than 30 generations. Unlike clinical T2DM in which obesity commonly occurs, GK rats show similarity with humans in terms of polygenetic and multifactorial pathogenesis (Portha et al., 2009). Chronic inflammation has been found to be closely associated with diabetic status in GK rats (Almon et al., 2009; Xue et al., 2011). Thus GK rats should be a suitable rodent model for assessing diabetes progression especially when evaluating the roles of chronic inflammation.

Salsalate, a nonacetylated prodrug of salicylate, has shown potential for decreasing blood glucose concentrations by decreasing inflammation in several clinical studies (Koska et al., 2009; Goldfine et al., 2010). However, the effects of salsalate on diabetes disease progression have not been investigated. Our study assesses the potential effect of salsalate on diabetes progression in GK rats. In addition, chronic inflammation is closely associated with an enlarged body mass and reducing inflammation might influence weight gain. Thus, another aim of our study is to explore the influence of salsalate on weight gain and energy expenditure.

Materials and Methods

Animals

Twelve 4-week-old male GK rats were obtained from Taconic Farms (Germantown, NY). Twelve age-matched male Wister-Kyoto (WKY) rats were purchased from Harlan (Indianapolis, IN) and served as controls. All rats were maintained on a strict 12-h light/12-h dark cycle and had free access to food and water. Blood glucose was measured once a week (Wednesday 9:00 AM). Body weight and food intake were measured every other day. To minimize animal stress, salsalate was formulated into the diet rather than giving the drug as an oral gavage. To get the daily profile of salicylate concentrations, blood was collected via the tail vein into capillary tubes (45 μl) once a week with collection times randomized at 2:00 AM, 8:00 AM, 8:00 PM, and noon (Friday). All animal studies were approved by the Institutional Animal Care and Use Committee of the University at Buffalo.

Diet

All rats were acclimatized for 1 week and fed a control diet (AIN-76A with bacon flavor; TestDiet, Richmond, IN), which included 18.0% protein, 5.0% fat, and 65.4% carbohydrate and had a digestible energy content of 3.77 kcal/g, with approximately 70% energy from carbohydrates. Salsalate (1000 ppm) was formulated to produce the salsalate-containing diet and used to feed rats from 5 weeks of age to the end of the experiment. The 12 GK rats and 12 WKY rats were randomly assigned to control diet-fed ($n = 6$) and salsalate-fed groups ($n = 6$). Diet was changed every other day, and leftover diets were measured to assess food intake. The food intake × salasalate concentration was used to calculate salsalate dosages.

Glucose and Salicylate Assays

Blood glucose was measured using a BD Logic blood glucose meter (BD Medical, Franklin Lakes, NJ). Blood salicylate was measured using a previously reported high-performance liquid chromatography method (Harrison et al., 1980) with minor modifications by lowering the mobile flow rate from 2.0 to 1.5 ml/min for system protection. The quantification limit was 1.6 μg/ml for both salsalate and salicylic acid with less than 10% intrabatch variability.

Models

Salicylate Pharmacokinetics. As a consequence of the gradual reduction of food intake with aging, the blood concentrations of salicylic acid declined and the pooled profile was characterized using:

$$dC_b/dt = C_0 - C_{max} \cdot t/(T_{50} + t) \quad (1)$$

where C_b is salicylate blood concentration, C_0 is the initial concentration at the beginning of feeding, C_{max} represents the maximum decrease of blood concentration with aging, and T_{50} is the time at which salicylate concentrations decreased by half of the maximum.

Disease Progression Model. The GK rats are a spontaneous diabetic model that is characterized by moderate insulin resistance (Bisbis et al., 1993), impaired glucose-induced insulin secretion (Portha et al., 1991), and progressive loss of β-cell function (Movassat et al., 1997). Insulin resistance and impaired β-cell function are both early events that contribute to the onset of diabetes in GK rats. Insulin resistance is found to be moderate and did not deteriorate with aging (Berthelier et al., 1997). Progressive β-cell deterioration has been found as a primary defect contributing to the establishment of overt diabetes in GK rats (Movassat et al., 1997).

Based on these disease characteristics, insulin resistance and β-cell dysfunction were considered as two main disease components in modeling the diabetes progression in GK rats. Figure 1 depicts the general schematic for the disease progression model integrated with salicylate pharmacodynamics. Blood glucose concentrations were characterized by using an indirect response model (Dayneka et al., 1993). Because we measured fed glucose concentrations, the main regulation of glucose by insulin is enhancing glucose utilization in peripheral tissues rather than inhibition of glucose production by liver. Therefore, two assumptive disease elements were incorporated to inhibit glucose utilization and are described by

$$\frac{dGlu}{dt} = k_{in\_glu} - Glu \cdot k_{out\_glu} \cdot (1 - S_{in} \cdot BF_m)$$

$$Glu(0) = k_{in\_glu}/k_{out\_glu} \quad (2)$$

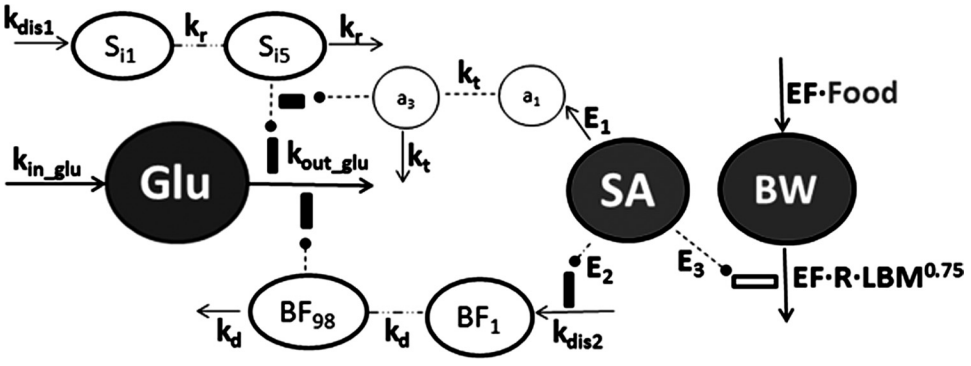

Fig. 1. Diabetes progression model with pharmacodynamics of salsalate and a growth model with salsalate effects. Symbols are defined under *Materials and Methods* and in Tables 2 and 3. Lines with arrows indicate conversion to or turnover of the indicated factors. Dashed lines ending in closed circles indicate an action is exerted by the connected factors. Dashed lines indicate transduction cascades.

where *Glu* represents blood glucose concentration. Glucose is produced by the zero-order rate constant k_{in_glu}, including absorption from nutrition and gluconeogenesis by the liver, k_{out_glu} is the first-order utilization rate constant by peripheral tissues, S_{in} and BF_m are two assumed disease components, S_{in} is progressive worsening of insulin resistance, and BF_m represents gradual deterioration of β-cell function. The two factors multiply each other to jointly reduce glucose utilization. The initial condition of *Glu* is *Glu*(0), which was estimated.

Two transduction cascades are applied to mimic gradual occurrence of two critical disease elements. Age-related development of insulin resistance is described by a function of S_{in} with a series of transit compartments that is initiated by a disease factor constant k_{dis1}. All compartments in this transduction cascade are described by differential equations that maintain homeostasis when unperturbed. The worsening process of insulin resistance is described by

$$\frac{dS_{i1}}{dt} = k_{dis1} - S_{i1} \cdot k_r \quad S_{i1}(0) = 0 \tag{3}$$

$$\frac{dS_{in}}{dt} = k_r \cdot (S_{i(n-1)} - S_{in}) \quad S_{in}(0) = 0 \tag{4}$$

where S_{in} indicates the nth transit compartment relevant to the series of events of insulin resistance that take place before the increase in blood glucose. The value of k_r indicates the turnover rate constant for each compartment in this series. The initial conditions for all transit compartments are 0, assuming no worsening of insulin resistance occurs before initiation by the disease factor k_{dis1}. Different transit compartment numbers were tested to find a number that sufficiently captured the glucose profile accounting for both a large delay and rapid rise to a new disease steady state. The interpretation of each compartment is not straightforward, and they are not components of a series of real events that occur during the disease process.

The β-cell dysfunction process was characterized similarly to that of insulin resistance. A series of transit compartments initiated by the disease factor constant k_{dis2} was used to describe the continuous change of β-cell dysfunction. The first and last transit compartments are:

$$\frac{dBF_1}{dt} = k_{dis2} - BF_1 \cdot k_d \quad BF_1(0) = 1 \tag{5}$$

$$\frac{dBF_m}{dt} = k_d \cdot (BF_{m-1} - BF_m) \quad BF_m(0) = 1 \tag{6}$$

where BF_m represents the nth transit compartment relevant to β-cell dysfunction and k_d is transduction rate constant. The transit compartment number was optimized to capture the data as best as possible. The initial conditions for all transit compartments were assumed to be 1 because this event happened later than insulin resistance and no influence was considered before the initiation of β-cell deterioration.

One important clarification about the two disease factors is that both S_i and BF_i represent a disease-worsening process and predisposed disease is not accounted for in this model. Thus, $S_i = 0$ or $BF_i = 1$ represents no worsening of disease compared with the starting time of the experiment (4 weeks of age), rather than no abnormality being present at that time.

Salicylate Pharmacodynamics. To integrate salicylate effects into the diabetes progression model, different approaches were tested, including modifying the transduction rate constants, reducing the disease factor constants k_{dis1} and k_{dis2}, and trying different combinations of both. The final model is shown in Fig. 1. Salicylate was assumed to ameliorate diabetes progression by decreasing both disease factors, in which a transduction model was used to describe the delayed protective effect on insulin resistance by salicylate and the suppressive effect on β-cell dysfunction was expressed by directly decreasing the disease factor k_{dis2}. The effect on insulin sensitivity was assumed to be linearly associated with salicylate concentrations. The protective effect on β-cell function was handled as a constant (E_2) because salicylate blood concentrations did not change much during the period of β-cell accelerated deterioration. The following equations describe the pharmacodynamics of salicylate on the diabetes progression in these GK rats:

$$\frac{dGlu}{dt} = k_{in\_glu} - Glu \cdot k_{out\_glu} \cdot (1 - S_{in}(d) \cdot BF_m(d))$$

$$Glu(0) = k_{in\_glu}/k_{out\_glu} \tag{7}$$

$$\frac{da_1}{dt} = C_b \cdot E_1 - a_1 \cdot k_t \quad a_1(0) = 0 \tag{8}$$

$$\frac{da_n}{dt} = k_t \cdot (a_{n-1} - a_n) \quad a_n(0) = 0 \tag{9}$$

$$S_{in}(d) = S_{in} \cdot (1 - a_n) \tag{10}$$

$$\frac{dBF_1(d)}{dt} = k_{dis2} \cdot (1 - E_2) - BF_1 \cdot k_d \quad BF_1(0) = 1 \tag{11}$$

$$\frac{dBF_m(d)}{dt} = k_d \cdot (BF_{m-1}(d) - BF_m(d)) \quad BF_m(0) = 1 \tag{12}$$

where $S_{in}(d)$ is the nth transit compartment that has been modified by salicylate and $BF_m(d)$ is the disease cascade of β-cell deterioration after salicylate treatment. All of the other parameters are identical to the diabetes progression model.

Growth Model. The mechanism-based growth model was originally developed by our laboratory based on the basic principles of physiology and biology (Landersdorfer et al., 2009). The complete model includes food intake, abdominal fat weights, and total body weight as well as leptin concentrations. The model applied in this study was derived from the original model with a simplification of the food intake component. Because leptin was not analyzed in this study, food intake was handled as a time-dependent variable rather than influenced by leptin concentrations. The model diagram is shown in Fig. 1. Body weight growth was described as:

$$dBW/dt = EF \cdot (Food - R \cdot (BW - Fat)^{0.75}) \quad BW(0) = BW_0 \tag{13}$$

where *Food* is food consumption per day (kcal/day), *BW* is body weight (g), *Fat* is total body fat, $BW - Fat$ represents an estimate for lean body mass (LBM), metabolic rate R is associated with allometrically scaled LBM derived from the equation by West et al. (2003), and *EF* is the efficiency of conversion of unmetabolized energy to body weight.

Previously, food intake was first found to increase and then slightly decrease with aging, but in this study no decreasing tendency was observed. The food intake was described with the equation (Madden, 1980) as:

$$\frac{dFood}{dt} = k_g \cdot (1 - Food/F_{max}) \quad Food(0) = F_0 \tag{14}$$

where k_g is the rate constant for increase in food intake and F_{max} is maximum food intake.

Total body fat was estimated from abdominal fat mass (Newby et al., 1990), which was captured by the Weibull function,

$$Fat = AFat \cdot 7.96 + 3.13 \tag{15}$$

$$AFat = AFat_m - (AFat_m - Bf) \cdot e^{-\left(\frac{cf-1}{cf}\right) \cdot \left(\frac{t}{IP}\right)^{cf}} \tag{16}$$

where *AFat* is abdominal fat mass, *Bf* and *cf* are constants and fixed, and *IP* is the inflection point of the *AFat* growth curve.

Parameter Variability and Observation Model. The interindividual variability was described by an exponential parameter variability model. The unidentified random variability was described by a combined additive and proportional error model for glucose, and only additive error model was used for food intake and body weight change.

Computation

The diabetes progression combined with salicylate effect was modeled using S-ADAPT (V1.56, beta; http://bmsr.usc.edu/Software/ADAPT/SADAPT-TRANsoftware.html) with the Monte Carlo Parametric Expectation Maximization algorithm. The SADAPT-TRAN translator tool was used to facilitate S-ADAPT analyses. The disease progression and pharmacodynamic model were fitted simultaneously. Body weight and food intake modeling was performed using NONMEM VI via the first-order conditional estimation method with interaction (NONMEM Project Group, University of California, San Francisco, CA). Body weight and food intake were fitted jointly. All parameters of the growth model were first estimated with independent typical values and intersubject variability for each group, and then combined if their estimates were similar among groups. Salicylate pharmacokinetics fitting was conducted using ADAPT 5 (Biomedical Simulations Resource, University of Southern California, Los Angeles, CA) with the maximum-likelihood method (D'Argenio and Schumitzky, 1997). The visual predictive check was performed using Berkeley Madonna (version 8.3.14; http://www.berkeleymadonna.com/) with 1000 times Monte Carlo simulation.

Competing models were compared by their objective function, predictive performance, parameter variability, and residual errors.

Results

Salicylate Pharmacokinetics. The parent drug salsalate concentrations were below the quantification limit for all blood samples collected during diet feeding, indicating salsalate was almost completely hydrolyzed into salicylic acid during absorption. Initially, we planned to describe daily salicylate profiles based on a two-compartment model with rat eating rates as an input. However, the high variability of rat eating behaviors made it challenging to describe daily profiles. Instead, we modeled salicylate pharmacokinetics by the naive pooling approach without considering the daily fluctuation. Daily changes were small and could be ignored for the long-term diabetes progression. The profiles of salicylate concentrations and fitted lines are shown in Fig. 2. Blood salicylate concentrations gradually declined over time and approached an apparent plateau approximately 14 weeks of age. Although the absolute amount of food intake increases with aging, the relative food intakes normalized by body weights decrease, leading to the decline in blood salicylate concentrations. Salicylate concentrations would increase if normalized by relative food intake (i.e., dose), suggesting that the systematic clearance of salicylate decreased with age, consistent with previous reports (Varma and Yue, 1984). The estimated parameters are listed in Table 1.

Glucose Dynamics. The changes in blood glucose concentrations are shown in Fig. 3. At 4 weeks of age, glucose concentrations are substantially higher in GK rats than in WKY rats, indicating that diabetes already exists before 4 weeks. No obvious glucose change was observed over time in WKY rats, in either control diet-fed or salsalate WKY rats. Glucose concentrations in GK rats showed a biphasic increase. The first phase started at approximately 5 weeks, resulting in a rise of glucose by 15 to 25 mg/dl, and the second phase appeared at 14 to 15 weeks with a glucose upsurge of more than 100 mg/dl. It is noteworthy that in the GK disease group the second phase was much higher in three rats than the others and diabetes seemingly showed two degrees of severity. Such severity was not handled separately in our model and was ascribed to interindividual variability. Salsalate significantly attenuated the glucose rise in both phases ($p < 0.05$; analysis of variance), producing nearly flat glucose profiles.

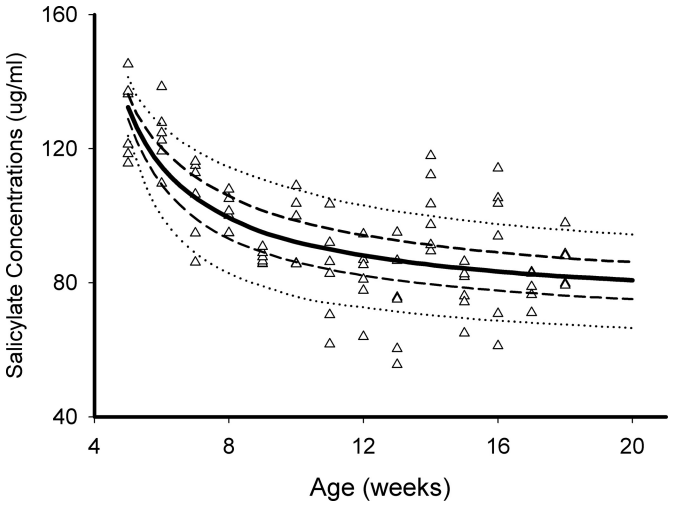

Fig. 2. Salicylate concentrations versus time profiles in salsalate-fed rats from 5 to 21 weeks of age: 5 to 95% percentile (dotted lines), 20 to 80% percentile (broken lines), and 50% percentile (solid line).

Disease Progression Model. The individual glucose profiles and model predictions are shown in Fig. 4. The biphasic profiles were reasonably captured by the disease progression model, in which the first phase was associated with insulin resistance and the second surge was related to the subsequent occurrence of β-cell deterioration. The optimized transit compartment number for insulin resistance cascade is 5 and for β-cell deterioration cascade it is 98. The two numbers were then fixed in the final model fitting. Final estimated parameters and between-subject variability are summarized in Table 2. All parameters were estimated with reasonable precision. Goodness-of-fit plots indicate the population method seems to considerably improve model fitting. The contributions to blood glucose changes from the two disease components can be estimated by the concentrations in the last transit compartments, shown as 0.091 (k_{dis1}/k_r) for insulin resistance and 3.76 (k_{dis2}/k_d) for β-cell deterioration. Based on the approach we formulated for describing disease progression with the two disease elements in eq. 2, k_{dis1} was estimated to account for 10% and k_{dis2} seemed to account for 60% of the glucose rise compared with initial glucose concentrations. The 49.7% intersubject variability of k_{dis2} indicates high individual variability of β-cell deterioration, corresponding to the high variability of the second phase. The predictive performance of the model, as shown in Fig. 4, is reasonable and adequately reflects the trend and variability of the raw data.

Salsalate Pharmacodynamics. The pharmacodynamic parameters and interindividual variability are listed in Table 2. The ameliorative effect of salsalate on diabetes progression was sufficiently described by the present model. Other models that were tried to incorporate salsalate effects in other

TABLE 1
Parameter estimates obtained from the time profiles of salicylate after feeding salsalate to rats from 5 to 21 weeks of age

Parameter	Definition	Estimate	SE%
C_0, μg/ml	Initial blood concentration of salicylate	132	3.85
C_{max}, μg/ml	Maximum decrease of salicylate concentrations	60.6	10.8
T_{50}, week	Time to decline half-maximally	7.52	40.7

SE%, relative standard error.

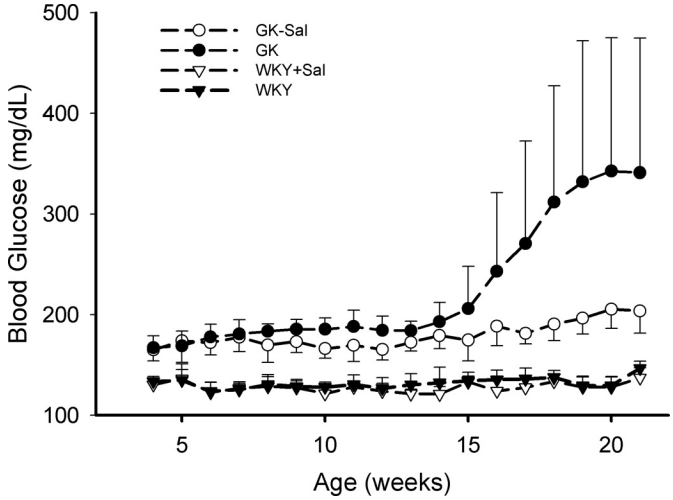

Fig. 3. Time course of blood glucose concentrations in GK and WKY rats from 4 to 21 weeks of age. GK, GK control rats; GK-Sal, salsalate-fed GK rats; WKY, WKY control rats; WKY-Sal, salsalate-fed WKY rats. Data are reported as mean ± S.D.

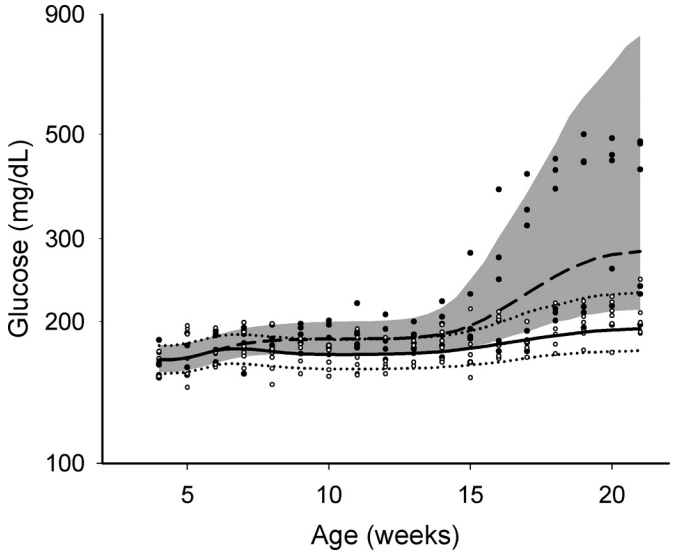

Fig. 4. Visual predictive check for blood glucose with aging for GK rats. Experimental measurement for natural disease group (●) and salsalate-fed group (○): 10 to 90% percentile (shaded area) and 50% percentile (dashed line) for the natural disease group; 10 to 90% percentile (dotted lines), and 50% percentile (solid line) for the salsalate-fed group.

ways did not generate good fittings or resulted in imprecise parameter estimates. The suppressive fractions of salsalate on two disease factors were calculated and the fraction on insulin resistance was estimated as 0.62 ($C_b \cdot E_1/k_t$) and on β-cell deterioration as 0.14 (E_2). As indicated in Table 2, intersubject variability was not precisely estimated for E_1, k_d, and k_t, which may be related to insufficient sample size and high intersubject variability. Even so, as shown in Fig. 4, the pharmacodynamic model provides a satisfactory predictive performance by visual predictive checks.

Simulation profiles of the two disease components are shown in Fig. 5. The onset of salsalate effect on insulin resistance is approximately 1.5 weeks after treatment. Because of the decline of salicylate concentrations over time, the suppressive effect slightly decreased after 9 weeks of age for disease factors 1. The accelerated deterioration of β-cell function appeared at approximately 14 to 16 weeks, and salsalate showed moderate improvement on β-cell deterioration.

Growth Model. The individual observed body weights and predicted curves are shown in Fig. 6. The parameters for the growth model are listed in Table 3. Body weights at the start of the study were similar for all groups. The control GK rats reached slighter higher body weights compared with salsalate-fed GK rats, despite similar energy intake. Assuming all GK rats require the same energy, the predicted body weights are still higher in control than salsalate groups, suggesting that energy intake alone cannot account for all the growth differences. The efficiency of converting energy (*EF*), which is not transformed to body weight was considerably higher in GK rats than in WKY rats, in line with our previous report (Landersdorfer et al., 2009). The metabolic rate (R) per gram of $LBM^{0.75}$ was significantly greater in salsalate-fed GK rats than control GK rats ($p < 0.05$), and all GK rats showed slightly higher R than WKY rats. The R of LBM was also higher in salsalate-fed WKY rats than control WKY rats, suggesting that the effect of enhancing R of LBM by salicylate was not limited to GK strains.

Observed energy intake and the predicted curves are shown in Fig. 7. Energy intakes were slightly lower in salsalate treatment groups for both GK and WKY rats. Maximum food intakes were estimated higher in GK rats than WKY rats, which is inconsistent with previous findings. Two reasons might account for this. One might be related to the different sources of WKY rats. Another explanation might be the different tasting propensity between GK and WKY rats, because the present diet had distinctive compositions and bacon flavor was formulated for better taste.

Three WKY rats were excluded from this analysis, two from the salsalate-fed group, one from the control group. These rats were suspected to have gastrointestinal tumors by visual check at the end of experiment. The reason for this is not quite clear, but it is not related to salsalate treatment.

Discussion

Disease progression models that integrate the underlying biological processes are increasingly used for understanding disease pathogenesis and evaluating drugs. A number of modeling efforts have been reported for diabetes disease progression. De Gaetano et al. (2008) provided a chronic diabetes progression model based on gradual worsening of insulin sensitivity and β-cell function. However, such a model was

TABLE 2
Parameter estimates for the diabetes progression model and salicylate pharmacodynamics

Parameter	Definition	Estimate	SE%	IIV%	SE%
k_{in_glu}, mg/dl/week	Glucose production rate	223	0.527	55.7	332
k_{out_glu}, 1/week	Glucose elimination rate	1.34	0.87	0.451	70.4
k_r, 1/week	Transduction rate for dis1	4.73	17.8	37.7	793
k_d, 1/week	Transduction rate for dis2	8.56	4.76	12.3	398
k_{dis1}, 1/week	Disease factor 1: insulin resistance	0.429	11.9	5.68	71.5
k_{dis2}, 1/week	Disease factor 2: β-cell deterioration	32.2	19.2	49.7	253
k_t, 1/week	Transduction rate for salsalate effect	1.49	12.4	7.97	390
E_1, ml/μg/week	Salsalate efficacy index in disease factor 1	0.0116	34.9	4.62	793
E_2	Salsalate improvement in disease factor 2	0.136	70	25.6	71.7
SD, mg/dl	Additive residual error	3.03	111	N.A.	N.A.
CV	Proportional residual error	4.86%	37	N.A.	N.A

IIV%, inter-individual variability; N.A., not applicable.

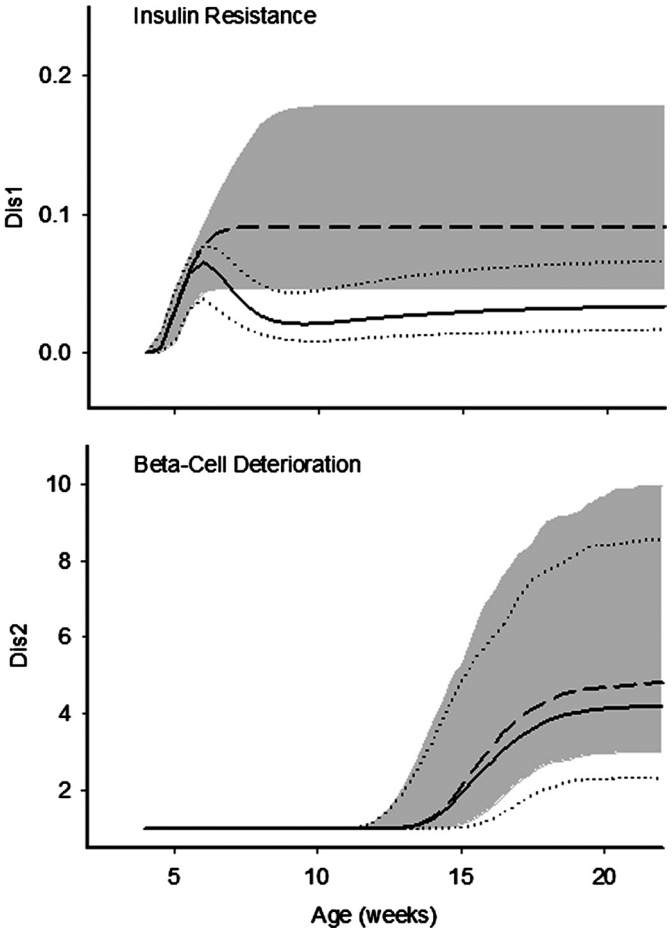

Fig. 5. Simulated time profiles of insulin resistance (top) and β-cell dysfunction (bottom) in natural disease and salsalate-fed groups. All symbols and lines are the same as in Fig. 4.

developed only for simulation and no experimental data were applied (De Gaetano et al., 2008). Topp et al., (2000) proposed a model incorporating insulin, glucose, and β-cells, and Ribbing et al. (2010) further implemented this model in clinical settings, which could be applied for a short period after diabetes diagnosis. In another model, two asymmetric equations were assumed to describe insulin resistance and β-cell dysfunction processes, which was applied in the evaluation of the clinical treatments (de Winter et al., 2006). Our former model that rationally factored in several disease components offered a decent description of the whole disease process from latent to overt diabetes in GK rats, wherein growth and maturation effects were also considered in comparison with normal WKY rats (Gao et al., 2011). This model indicated insulin resistance and β-cell dysfunction as the two critical components in GK rats' diabetes progression. The present model thus focuses on the two disease components by continuously measuring glucose from 4 to 21 weeks, as well as incorporating salsalate treatment to evaluate the potential involvement of inflammation on diabetes progression.

The pathogenesis of T2DM involves abnormalities in insulin action, β-cell function, and endogenous glucose output. For a long time, the sequence with which these abnormalities develop and their relative contributions to glucose tolerance were not quite clear. Recently, there was consensus that β-cell failure is a proximal defect in the process of developing glucose intolerance and leads to overt T2DM. Preservation of β-cell function shows good potential in the treatment of diabetes (Nyalakonda et al., 2010). Similar disease processes were observed in the GK rat. Although β-cell defects were already present at early times, substantial β-cell failure becomes evident only at 16 weeks of age (O'Rourke et al., 1997; Gao et al., 2011). Shown in our results, the sharp rise of glucose appeared at approximately 14 to 16 weeks (Fig. 3), consistent with the reported time of substantial β-cell deterioration. Therefore, it is rational to assume that disease factor 2 that happens at approximately 15 weeks represents overt β-cell failure.

In GK rats, insulin resistance was found to be moderate and would not progressively deteriorate after 8 weeks (Berthelier et al., 1997). The time of occurrence of insulin resistance in GK rats is not clear in the literature. Standaert et al. (2004) implied systematic resistance had become obvious at 8 weeks, which was evident from the defects of several signaling components related to insulin action, such as insulin receptor substrate 1, α-protein kinase C, and protein kinase B. As reported by Ueta et al. (2005), systematic insulin resistance was already evident at 4 weeks and no more deterioration was found until 26 weeks. Mild hyperinsulinemia before overt diabetes also suggests the state of insulin resistance, which was observed at 8 weeks of age in GK rats from our previous study (Gao et al., 2011). Collectively, although not being a primary defect of diabetes in GK rats, insulin resistance is an important factor contributing to glucose intolerance before overt diabetes. As shown in Fig. 5, insulin resistance appeared at 4 to 5 weeks and contributed to the first phase of increased glucose, consistent with previous observations that insulin resistance developed before overt hyperglycemia.

Functional adaptation between insulin resistance and

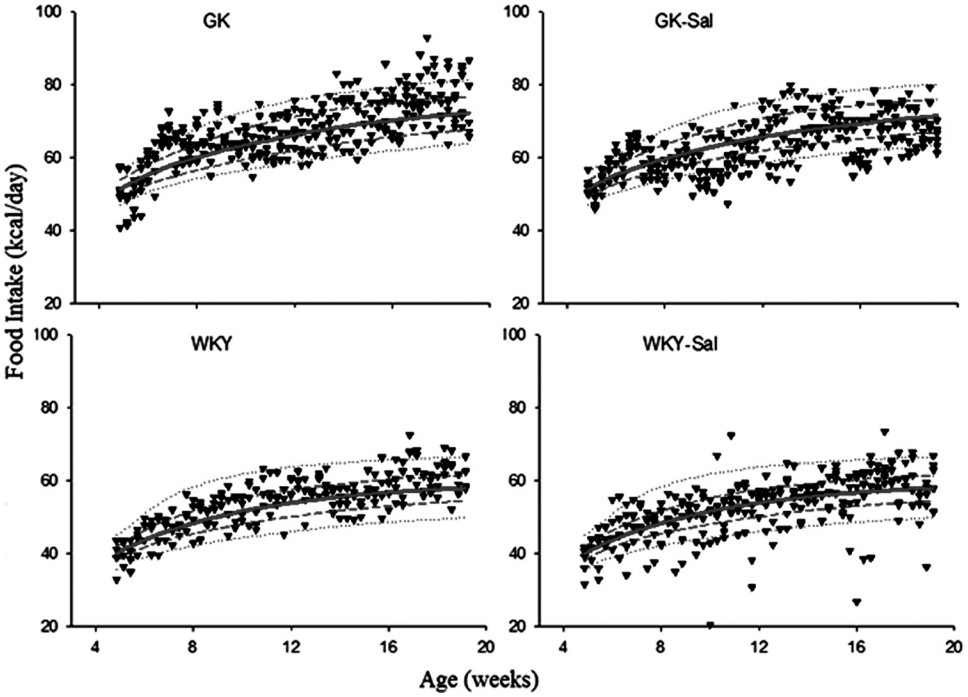

Fig. 6. Food intake versus age for the four groups of rats: 10 to 90% percentile (dotted lines), 25 to 75% percentile (broken lines), and 50% percentile (solid lines).

TABLE 3
Parameter estimates for the mechanism-based growth model in four groups

Parameter	Group	Definition	Estimate	SE%	IIV%	SE%
k_g, kcal/day/day	All rats	Food intake increasing rate	1.36	12.1	70.6	38
F_{max}, kcal/day	GK-Sal	Maximum food intake	77	4.2	7.71	4.2
F_{max}, kcal/day	GK-N	Maximum food intake	78.2	4.6	7.71	4.2
F_{max}, kcal/day	WKY-Sal	Maximum food intake	66	3.7	7.71	4.2
F_{max}, kcal/day	WKY-N	Maximum food intake	61	2	7.71	4.2
$AFat_m$, g	GK	Maximum abdominal fat mass	31.6	17.2	27.6	101
$AFat_m$, g	WKY	Maximum abdominal fat mass	19.4	26.4	27.6	101
BW_0, g	All rats	Body weight at start of study (4 weeks of age)	120	2.2	9.24	25.9
EF, g/kcal	GK	Efficacy to convert energy that is not needed for metabolism to body weight	0.243	4.2	N.A.	N.A.
EF, g/kcal	WKY	Efficacy to convert energy that is not needed for metabolism to body weight	0.215	10.8	N.A.	N.A.
R, kcal/day/g $LBM^{0.75}$	GK-Sal	Metabolic rate per $LBM^{0.75}$	1.18	3.0	5.39	66.7
R, kcal/day/g $LBM^{0.75}$	GK-N	Metabolic rate per $LBM^{0.75}$	1.03	6.7	5.39	66.7
R, kcal/day/g $LBM^{0.75}$	WKY-Sal	Metabolic rate per $LBM^{0.75}$	1.03	10.5	5.39	66.7
R, kcal/day/g $LBM^{0.75}$	WKY	Metabolic rate per $LBM^{0.75}$	0.927	9.4	5.39	66.7
F_0, kcal/day	GK	Food intake at start of study (4 weeks of age)	51.5	3.3	7.13	4.6
F_0 , kcal/day	WKY	Food intake at start of study (4 weeks of age)	39.8	2.5	7.13	4.6
IP, day	All rats	Inflection point for abdominal fat growth curve	21.1	N.A.	N.A.	N.A.
$FERR$, kcal/day	All rats	Additive error for food intake	4.88	15.5		
$BWERR$, g	All rats	Additive error for body weight	3.62	14.0		

GK, GK control diet-fed rats; GK-Sal, salsalate-fed GK rats; WKY, WKY control diet-fed rats; WKY-Sal, salsalate-fed WKY rats; IIV%, inter-individual variability; N.A., not applicable.

β-cell function has been widely investigated in human T2DM. Nonetheless, it has not been well established in GK rats. As known in GK rats, the glucose-induced insulin response is impaired and resistance may not effectively trigger more insulin secretion if glucose mediates this compensation. The degree of adaptation in GK rats might not be as high as in clinical settings because of the early defect of β-cells and impaired glucose response. For simplicity, the present model did not include this compensation and the two disease elements were treated independently.

Accumulating evidence suggests an inflammatory process, characterized by local cytokine/chemokine production and immune cell infiltration, is involved in regulating islet dysfunction and insulin resistance in T2DM. The initiation of the chronic inflammation is still unclear but current research supports chronic inflammation associated with enlarged body fat mass (Das and Mukhopadhyay, 2011). Our recent studies in GK rats demonstrated chronic inflammation was also present systemically and in liver, skeletal muscle, and adipose tissue (Almon et al., 2009; Nie et al., 2011; Xue et al., 2011). The studies by another group reported that GK islets exhibited increased mRNA for numerous islet cytokines, chemokines, and cytokine signaling intermediates (Ehses et al., 2009b; Lacraz et al., 2009). The source of chronic inflammation in GK rats is still inconclusive but one thing that is apparent is that the inflammation is not fat driven because GK rats are a diabetic model exhibiting a nonobese phenotype. Therefore, one of our objectives in this study was to test the hypothesis that chronic inflammation regardless of source plays a causal role in T2DM. As indicated in Fig. 3,

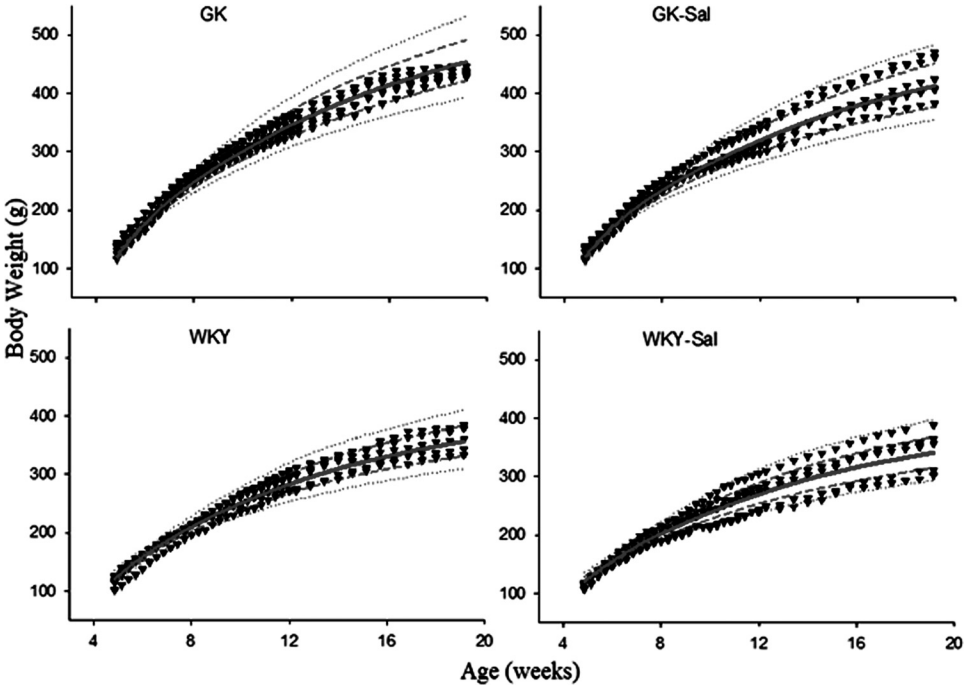

Fig. 7. Body weight increase versus age for the four groups of rats. All symbols and lines are the same as in Fig. 6.

although salsalate did not completely normalize hyperglycemia, it remarkably ameliorated diabetes progression and resulted in a flattened glucose profiles. Given the well established anti-inflammatory effects of salsalate, our results imply that inflammation plays an important role in the pathogenesis of diabetes in GK rats. Studies by Ehses et al. (2009b) were supportive of our conclusion, as they found that lowering chronic inflammation by IL-1Ra ameliorated hyperglycemia in GK rats and the improvements were paralleled by reducing inflammatory mediators in islet and peripheral tissues.

Several studies have indicated that salsalate inhibits activity of transcription factor NF-κB, which regulates the generation of multiple inflammatory factors. NF-κB activity is also found to be inhibited by salicylate in diabetes models (Goldfine et al., 2008). Given higher expression of NF-κB in GK rats than in age-matched Wister rats (Lacraz et al., 2009), salsalate improves hyperglycemia in GK rats most likely by inhibiting NF-κB activity. In addition, IL-1β is a key activator of NF-κB, and IL-1β was found to contribute to β-cell death by activating NF-κB (Ortis et al., 2008); the benefit of IL-1Ra in GK rats infers the potential action of blocking NF-κB by salicylate. However, until now, no direct evidence was available concerning the underlying mechanism. Several clinical studies indicated that the additional mechanisms that might contribute to the glucose-lowering effects of salicylate include inhibition of cellular kinase (Frantz and O'Neill, 1995), increase in adiponectin concentrations, and lowering circulating triglyceride concentrations (Goldfine et al., 2010). Thus, salsalate may decrease glucose concentrations in multiple ways. Further studies are warranted.

The suppressive effects of salsalate on both disease components were quantitatively assessed, and predominant improvement of insulin resistance was suggested. Here, we speculate that salicylate in the GK rats might be more effective at reducing peripheral tissue inflammation than islet inflammation. Similar observations were obtained where lower doses of IL-1Ra showed benefit in insulin resistance, whereas high doses of IL-1Ra are required to effectively inhibit islet inflammation (Ehses et al., 2009b). The dose dependencies of these effects are not well elucidated in this study. Salicylate concentrations were considered for the insulin resistance cascade, but interpretation of the sensitivity constant (E_1) is cautioned because of the narrow range of salicylate concentrations. Several clinical trials also did not reflect any dose dependence of salsalate effects in clinical T2DM (Goldfine et al., 2008, 2010). Moreover, the insulin-sensitizing effect of IL-1Ra in GK rats was found to be U-shaped (Ehses et al., 2009b). There may be different levels and roles of inflammation in tissues that control diabetes progression.

Another issue addressed in the present study was the potential effect of salsalate on weight gain and energy expenditure in GK rats. Higher energy expenditure is expected in obesity or diabetes. The growth model indicated that a higher metabolic rate (R) was present in GK rats than age-matched WKY rats, consistent with previous observations (Landersdorfer et al., 2009). Salsalate was suggested to enhance R and resulted in lower body weight compared with the control group. Such an effect of salsalate was present in both GK and WKY rats, indicating the action is independent of diabetic status. Similar effects were seen clinically that salsalate stimulated whole body energy expenditure by increasing oxidative glucose disposal, which might be attributed to elevated blood insulin concentrations (Meex et al., 2011). The positive effects of salsalate on energy expenditure should augment hypoglycemia treatments with weight gain problems.

Conclusions

The proposed model satisfactorily captured the biphasic glucose rise in GK rats from 4 to 21 weeks of age by assuming two disease cascades to mimic insulin resistance and β-cell dysfunction. Salsalate substantially ameliorated diabetes progression and resulted in flat glucose profiles. Our model

incorporates anti-inflammatory effects in the characterization of diabetes progression. Expanding this model by including specific inflammatory factors will be beneficial in gaining further understanding of the causal role of inflammation on diabetes progression and in designing related pharmacological studies.

Acknowledgments

We thank Suzette M. Mis and Nancy A. Pyszczynski for technical assistance.

Authorship Contributions

Participated in research design: Cao, DuBois, Almon, and Jusko.
Conducted experiments: Cao, DuBois, and Sun.
Performed data analysis: Cao and Jusko.
Wrote or contributed to the writing of the manuscript: Cao, DuBois, Almon, and Jusko.

References

Almon RR, DuBois DC, Lai W, Xue B, Nie J, and Jusko WJ (2009) Gene expression analysis of hepatic roles in cause and development of diabetes in Goto-Kakizaki rats. *J Endocrinol* **200:**331–346.
Berthelier C, Kergoat M, and Portha B (1997) Lack of deterioration of insulin action with aging in the GK rat: a contrasted adaptation as compared with nondiabetic rats. *Metabolism* **46:**890–896.
Bisbis S, Bailbe D, Tormo MA, Picarel-Blanchot F, Derouet M, Simon J, and Portha B (1993) Insulin resistance in the GK rat: decreased receptor number but normal kinase activity in liver. *Am J Physiol Endocrinol Metab* **265:**E807–E813.
D'Argenio DZ and Schumitzky A (2009) ADAPT V User's Guide: Pharmacokinetic/Pharmacodynamic System Analysis Software, Biomedical Simulations Resource, Los Angeles, CA.
Das A and Mukhopadhyay S (2011) The evil axis of obesity, inflammation and type-2 diabetes. *Endocr Metab Immune Disord Drug Targets* **11:**23–31.
Dayneka NL, Garg V, and Jusko WJ (1993) Comparison of four basic models of indirect pharmacodynamic responses. *J Pharmacokinet Biopharm* **21:**457–478.
De Gaetano A, Hardy T, Beck B, Abu-Raddad E, Palumbo P, Bue-Valleskey J, and Pørksen N (2008) Mathematical models of diabetes progression. *Am J Physiol Endocrinol Metab* **295:**E1462–E1479.
de Winter W, DeJongh J, Post T, Ploeger B, Urquhart R, Moules I, Eckland D, and Danhof M (2006) A mechanism-based disease progression model for comparison of long-term effects of pioglitazone, metformin and gliclazide on disease processes underlying Type 2 Diabetes Mellitus. *J Pharmacokinet Pharmacodyn* **33:**313–343.
Donath MY, Böni-Schnetzler M, Ellingsgaard H, and Ehses JA (2009) Islet inflammation impairs the pancreatic β-cell in type 2 diabetes. *Physiology (Bethesda)* **24:**325–331.
Ehses JA, Ellingsgaard H, Böni-Schnetzler M, and Donath MY (2009a) Pancreatic islet inflammation in type 2 diabetes: from α and β cell compensation to dysfunction. *Arch Physiol Biochem* **115:**240–247.
Ehses JA, Lacraz G, Giroix MH, Schmidlin F, Coulaud J, Kassis N, Irminger JC, Kergoat M, Portha B, Homo-Delarche F, et al. (2009b) IL-1 antagonism reduces hyperglycemia and tissue inflammation in the type 2 diabetic GK rat. *Proc Natl Acad Sci U S A* **106:**13998–14003.
Frantz B and O'Neill EA (1995) The effect of sodium salicylate and aspirin on NF-κB. *Science* **270:**2017–2019.
Gao W, Bihorel S, DuBois DC, Almon RR, and Jusko WJ (2011) Mechanism-based disease progression modeling of type 2 diabetes in Goto-Kakizaki rats. *J Pharmacokinet Pharmacodyn* **38:**143–162.
Gobburu JV and Lesko LJ (2009) Quantitative disease, drug, and trial models. *Annu Rev Pharmacol Toxicol* **49:**291–301.
Goldfine AB, Fonseca V, Jablonski KA, Pyle L, Staten MA, Shoelson SE, and TINSAL-T2D (Targeting Inflammation Using Salsalate in Type 2 Diabetes) Study Team (2010) The effects of salsalate on glycemic control in patients with type 2 diabetes: a randomized trial. *Ann Intern Med* **152:**346–357.
Goldfine AB, Silver R, Aldhahi W, Cai D, Tatro E, Lee J, and Shoelson SE (2008) Use of salsalate to target inflammation in the treatment of insulin resistance and type 2 diabetes. *Clin Transl Sci* **1:**36–43.
Harrison LI, Funk ML, and Ober RE (1980) High-pressure liquid chromatographic determination of salicylsalicylic acid, aspirin, and salicylic acid in human plasma and urine. *J Pharm Sci* **69:**1268–1271.
Koska J, Ortega E, Bunt JC, Gasser A, Impson J, Hanson RL, Forbes J, de Courten B, and Krakoff J (2009) The effect of salsalate on insulin action and glucose tolerance in obese non-diabetic patients: results of a randomised double-blind placebo-controlled study. *Diabetologia* **52:**385–393.
Lacraz G, Giroix MH, Kassis N, Coulaud J, Galinier A, Noll C, Cornut M, Schmidlin F, Paul JL, Janel N, et al. (2009) Islet endothelial activation and oxidative stress gene expression is reduced by IL-1Ra treatment in the type 2 diabetic GK rat. *PLoS One* **4:**e6963.
Landersdorfer CB, DuBois DC, Almon RR, and Jusko WJ (2009) Mechanism-based modeling of nutritional and leptin influences on growth in normal and type 2 diabetic rats. *J Pharmacol Exp Ther* **328:**644–651.
Larsen CM, Faulenbach M, Vaag A, Vølund A, Ehses JA, Seifert B, Mandrup-Poulsen T, and Donath MY (2007) Interleukin-1-receptor antagonist in type 2 diabetes mellitus. *N Engl J Med* **356:**1517–1526.
Madden LV (1980) Quantification of disease progression. *Prot Ecol* **2:**159–176.
Marchetti P, Del Prato S, Lupi R, and Del Guerra S (2006) The pancreatic β-cell in human type 2 diabetes. *Nutr Metab Cardiovasc Dis* **16(Suppl 1):**S3–S6.
Meex RC, Phielix E, Moonen-Kornips E, Schrauwen P, and Hesselink MK (2011) Stimulation of human whole-body energy expenditure by salsalate is fueled by higher lipid oxidation under fasting conditions and by higher oxidative glucose disposal under insulin-stimulated conditions. *J Clin Endocrinol Metab* **96:**1415–1423.
Movassat J, Saulnier C, Serradas P, and Portha B (1997) Impaired development of pancreatic β-cell mass is a primary event during the progression to diabetes in the GK rat. *Diabetologia* **40:**916–925.
Newby FD, DiGirolamo M, Cotsonis GA, and Kutner MH (1990) Model of spontaneous obesity in aging male Wistar rats. *Am J Physiol Regul Integr Comp Physiol* **259:**R1117–R1125.
Nie J, Xue B, Sukumaran S, Jusko WJ, Dubois DC, and Almon RR (2011) Differential muscle gene expression as a function of disease progression in Goto-Kakizaki diabetic rats. *Mol Cell Endocrinol* **338:**10–17.
Nyalakonda K, Sharma T, and Ismail-Beigi F (2010) Preservation of β-cell function in type 2 diabetes. *Endocr Pract* **16:**1038–1055.
Olefsky JM and Glass CK (2010) Macrophages, inflammation, and insulin resistance. *Annu Rev Physiol* **72:**219–246.
O'Rourke CM, Davis JA, Saltiel AR, and Cornicelli JA (1997) Metabolic effects of troglitazone in the Goto-Kakizaki rat, a non-obese and normolipidemic rodent model of non-insulin-dependent diabetes mellitus. *Metabolism* **46:**192–198.
Ortis F, Pirot P, Naamane N, Kreins AY, Rasschaert J, Moore F, Théâtre E, Verhaeghe C, Magnusson NE, Chariot A, et al. (2008) Induction of nuclear factor-κB and its downstream genes by TNF-α and IL-1β has a pro-apoptotic role in pancreatic β cells. *Diabetologia* **51:**1213–1225.
Portha B, Lacraz G, Kergoat M, Homo-Delarche F, Giroix MH, Bailbé D, Gangnerau MN, Dolz M, Tourrel-Cuzin C, and Movassat J (2009) The GK rat β-cell: a prototype for the diseased human β-cell in type 2 diabetes? *Mol Cell Endocrinol* **297:**73–85.
Portha B, Serradas P, Bailbé D, Suzuki K, Goto Y, and Giroix MH (1991) β-Cell insensitivity to glucose in the GK rat, a spontaneous nonobese model for type II diabetes. *Diabetes* **40:**486–491.
Ribbing J, Hamrén B, Svensson MK, and Karlsson MO (2010) A model for glucose, insulin, and β-cell dynamics in subjects with insulin resistance and patients with type 2 diabetes. *J Clin Pharmacol* **50:**861–872.
Standaert ML, Sajan MP, Miura A, Kanoh Y, Chen HC, Farese RV Jr, and Farese RV (2004) Insulin-induced activation of atypical protein kinase C, but not protein kinase B, is maintained in diabetic (ob/ob and Goto-Kakazaki) liver. Contrasting insulin signaling patterns in liver versus muscle define phenotypes of type 2 diabetic and high fat-induced insulin-resistant states. *J Biol Chem* **279:**24929–24934.
Topp B, Promislow K, deVries G, Miura RM, and Finegood DT (2000) A model of β-cell mass, insulin, and glucose kinetics: pathways to diabetes. *J Theor Biol* **206:**605–619.
Ueta K, Ishihara T, Matsumoto Y, Oku A, Nawano M, Fujita T, Saito A, and Arakawa K (2005) Long-term treatment with the Na+-glucose cotransporter inhibitor T-1095 causes sustained improvement in hyperglycemia and prevents diabetic neuropathy in Goto-Kakizaki rats. *Life Sci* **76:**2655–2668.
Varma DR and Yue TL (1984) Influence of age, sex, pregnancy and protein-calorie malnutrition on the pharmacokinetics of salicylate in rats. *Br J Pharmacol* **82:**241–248.
Wellen KE and Hotamisligil GS (2005) Inflammation, stress, and diabetes. *J Clin Invest* **115:**1111–1119.
West GB, Savage VM, Gillooly J, Enquist BJ, Woodruff WH, and Brown JH (2003) Physiology: why does metabolic rate scale with body size? *Nature* **421:**713; discussion 714.
Xue B, Sukumaran S, Nie J, Jusko WJ, Dubois DC, and Almon RR (2011) Adipose tissue deficiency and chronic inflammation in diabetic Goto-Kakizaki rats. *PLoS One* **6:**e17386.

Address correspondence to: Dr. William J. Jusko, Department of Pharmaceutical Sciences, 565 Hochstetter Hall, State University of New York, Buffalo, NY 14260. E-mail: wjjusko@buffalo.edu